doi:10.19691/j.cnki.1004–4493.2024.03.002

The Influence of Biomass Cokes on the Microstructure and Thermal Shock Resistance of MgO–C Refractories

Patrick GEHRE[1*], Magzhan KAPESSOV[1], Stefan GUHL[2], Martin GRÄBNER[2], Christos G. ANEZIRIS[1]

1 Institute of Ceramics, Refractories and Composite Materials, TU Bergakademie Freiberg, Freiberg 09599, Germany

2 Institute of Energy Process Engineering and Chemical Engineering, TU Bergakademie Freiberg, Freiberg 09599, Germany

Patrick Gehre studied ceramic, glass and construction materials at TU Bergakademie Freiberg (Germany). Since 2008, he has been a research associate at the Institute of Ceramics, Refractories and Composite Materials, where he earned his PhD in 2013 and postdoctoral lecture qualification in 2021. Since 2015, he has been a chief engineer and leads the group of ceramic technologies. His research interests focus on the thermomechanical properties and the microstructure of shaped and unshaped alumina- and magnesia-based refractories with attention to the thermal shock resistance and corrosion resistance as well as the flame spraying technology.

Abstract

In this study, biomass cokes from sunflower seed hull (SFSH) and wood pellets (WP) were added to a MgO–C batch (3 *mass*% C) to replace 1.1 *mass*% of graphite. After hardening and carbonizing the samples, the influence of the biomass cokes on the microstructure and thermal shock resistance was investigated. The replacement of flaky graphite by carbonized WP and SFSH reduced the bulk density and increased the apparent porosity after pressing and carbonization, but the degree was only marginal. This was confirmed by SEM investigations, where the biomass-coke containing samples exhibited a microstructure with a higher amount of pores between the fine MgO grains. The thermal shock resistance of the porous wood pellet coke containing MgO–C is at the same level as the reference sample but not superior to it.

Key words: MgO–C; carbon; biomass; microstructure; thermal shock

1 Introduction

MgO–C refractories are the dominating lining materials in steel-making and refining plants such as basic oxygen furnaces (BOF), electric arc furnaces (EAF), and steel ladles[1]. In these vessels, MgO–C bricks have to withstand aggressive steel/slag systems, thermal shocks, and high temperatures[2–4]. The MgO and carbon raw materials (sometimes including metallic powder as antioxidants) are bonded by a high carbon-containing pitch or resin binder system. The carbon portion plays a key role in the batches. With its high thermal conductivity and low thermal expansion, carbon provides the MgO–C brick an excellent thermal shock resistance. Additionally, the carbon bond concedes a flexible microstructure, which withstands a higher degree of thermal stresses. Carbon also reduces the corrosion of the brick as it is poorly wetted by steel and slag. Finally, yet importantly, carbon is a valued pressing aid for the production of MgO–C bricks significantly reducing their apparent porosity in comparison to fired MgO bricks.

The refractory industry is by far the largest consumer of natural graphite, accounting for approximately 46% of global consumption of 947 000 t in 2018[5]. Recent investigations showed an improvement in MgO–C bricks by partially replacing flaky graphite with expanded graphite (EG)[6–7]. However, the amount of EG is limited to less than 1 *mass*% due to its poor oxidation resistance. Carbon black (CB), another known carbon source for refractories, is also only used in limited amounts in MgO–C due to its low primary particle size, which increases the amount of liquid binder needed and reduces the oxidation resistance. However, CB enables an optimal pore filling resulting in higher corrosion resistance[8]. New types of MgO–C bricks, especially those with low C, contain nano carbon black (nCB), which favours the filling of tiny spaces, pores, and gaps in the matrix and thus improves a couple of properties[9–11].

The predicted surge in demand for graphite by the growing battery industry marks competition in raw material supply for the refractory industry. In this regard, CB was partially replaced by coke from wood and sunflower seed hull pellets, respectively, and

*Corresponding e-mail: patrick.gehre@ikfvw.tu-freiberg.de

the impact of the carbonized biomass on the properties of MgO–C such as the pore size distribution, phase composition, bulk density, apparent porosity, cold crushing strength (CCS), refractoriness under load (RuL), and oxidation resistance was investigated[12]. From the previous study, some questions are still unresolved. As carbon acts as a pressing aid and pore filler, one aim of the present study was a deeper investigation of the microstructure of MgO–C with biomass cokes. Additionally, due to the much higher porosity of the biomass cokes compared to common graphite and CB raw materials, the biomass coke containing MgO–C materials may have a better thermal shock resistance, which was investigated, too.

2 Experimental

MgO–C with flaky graphite and CB was prepared as reference materials. All batch variations contain 1.1 *mass*% carbon black as a fixed carbon source, whereas 1.1 *mass*% flaky graphite was replaced by the equal amount of carbonized wood (WP) and sunflower seed hull (SFSH) pellets, respectively. The compositions are displayed in Table 1. The in-house manufacturing of the biomass cokes, their elementary and proximate analysis, the chemical composition of their ash portion after carbonization, and the grain size are presented in the previous study[12].

Table 1 Compositions of MgO–C samples /*mass*%

Raw materials		MgO–C_NFL	MgO–C_WP	MgO–C_SFSH
Fused MgO	2–4 mm	17.0		
	1–2 mm	29.7		
	0–1 mm	34.3		
Sintered MgO powder		16.8		
Flaky graphite NFL		1.1	–	–
Carbon black N991		1.1		
Carbonized wood pellets		–	1.1	–
Carbonized sunflower seed hull pellets		–	–	1.1
Powder resin 0235 DP (extra adding)		1.5		
Liquid resin 9308-FL (extra adding)		1.5		
Hardener (extra adding)		0.3		

Next to the biomass cokes, the raw materials used for the preparation of the MgO–C samples were MgO with a purity of 98% (QMAG), flaky graphite NFL (min. 70%>160 μm, 87%–98% C, Graphit Kropfmühl AG), and carbon black MT Thermax N-991 Powder (<45 μm, 99.6% C, Lehmann & Voss & Co. KG). Liquid resin 9308-FL, powder resin 0235 DP, and hexamethylenetetramine hardener (all Hexion) were used as binders. After the mixing process, bar-shaped samples with a dimension of 150 mm×25 mm×25 mm were pressed with a uniaxial press and an applied pressure of 120 MPa. After pressing, the samples were hardened by a three-step thermal treatment with a maximum temperature of 180 °C and carbonized in an electrically heated furnace at 1 000 °C for 5 h using a coke bed.

To identify the impact of the biomass cokes compared to flaky graphite on the pressing behaviour of the batches, the bulk density and apparent porosity of the samples have been analysed after pressing and carbonization, respectively, according to EN 993-1 using toluol. The dynamic Young's modulus E was determined using the ultrasonic runtime method. The microstructure has been examined utilizing a digital light microscope (VHX-2000, Keyence) as well as an SEM equipped with EDS (Philips XL 30 ESEM FEG). The thermal shock resistance has been evaluated by determining the modulus of rupture (MOR) before and after shocking the samples from 950 °C to ambient temperature with pressurized air (0.1 MPa) for 5 min. During heating to the test temperature, the samples were embedded in coke to avoid oxidation.

3 Results and Discussion

3.1 Bulk Density and Apparent Porosity

Table 2 gives an overview of the bulk density (BD) and apparent porosity (AP) of the samples after pressing as well as after carbonization. Replacing natural flaky graphite with biomass cokes has a negative effect on the pressing of the batches and hence the physical properties of the pressed sample bars, as the BD decreases and the AP increases. This can be explained by the particle structure. Flaky graphite has a greasing effect caused by its lamellar structure, which is not the case for the grain-like biomass cokes. The biomass cokes with a d_{50} of 134.3 μm (WP) and 57.2 μm (SFSH)[12], respectively, are finer compared to graphite NFL (d_{50}>160 μm) and may fill finer pores. However, this effect is not reflected by a decreased apparent porosity. Most likely, the positive impact of the lubrication effect of graphite NFL during pressing superposes the pore-filling effect of the finer biomass-cokes, and/or the much finer carbon black, which is present in all compositions, has the main impact on the pore-filling. The worsening of the physical properties by replacing graphite with the biomass cokes remains after carbonization. However, the decrease in AP from 8.4% of the reference batch to *e.g.* 9.8% of the sample MgO–C_WP after pressing and from 15.8% to 16.7% after carbonization, respectively, is of little account.

Table 2 Bulk density and apparent porosity after pressing and carbonization at 1 000 °C

Samples	After pressing		After carbonization	
	Bulk density /(g · cm^{-3})	Apparent porosity /%	Bulk density /(g · cm^{-3})	Apparent porosity /%
MgO–C_NFL	3.02	8.4	2.91	15.8
MgO–C_WP	2.95	9.8	2.86	16.7
MgO–C_SFSH	2.94	10.5	2.88	16.4

3.2 Young's Modulus of Elasticity

The results of Young's modulus of elasticity (*E*) determination (Table 3) confirm the tendency gained by the detection of the bulk density. The use of graphite NFL results in denser samples with a higher *E* (81.5 GPa of sample MgO–C_NFL compared to 68.4 GPa of sample MgO–C_SFSH) after pressing. As expected, the *E* significantly decreases with the carbonization step resulting in a much porous microstructure for all samples. Especially in the case of sample MgO–C_SFSH, the replacement of graphite by the biomass coke does not negatively influence Young's modulus of elasticity after carbonization.

Table 3 Young's modulus of elasticity after pressing and carbonization at 1 000 °C

Samples	Young's modulus *E* /GPa	
	After pressing	After carbonization
MgO–C_NFL	81.5	4.3
MgO–C_WP	65.6	3.6
MgO–C_SFSH	68.4	4.6

3.3 Microstructure

Figure 1 displays the microstructure of the samples after pressing (Fig. 1 a, c, e) and carbonization (Fig. 1 b, d, f), respectively,

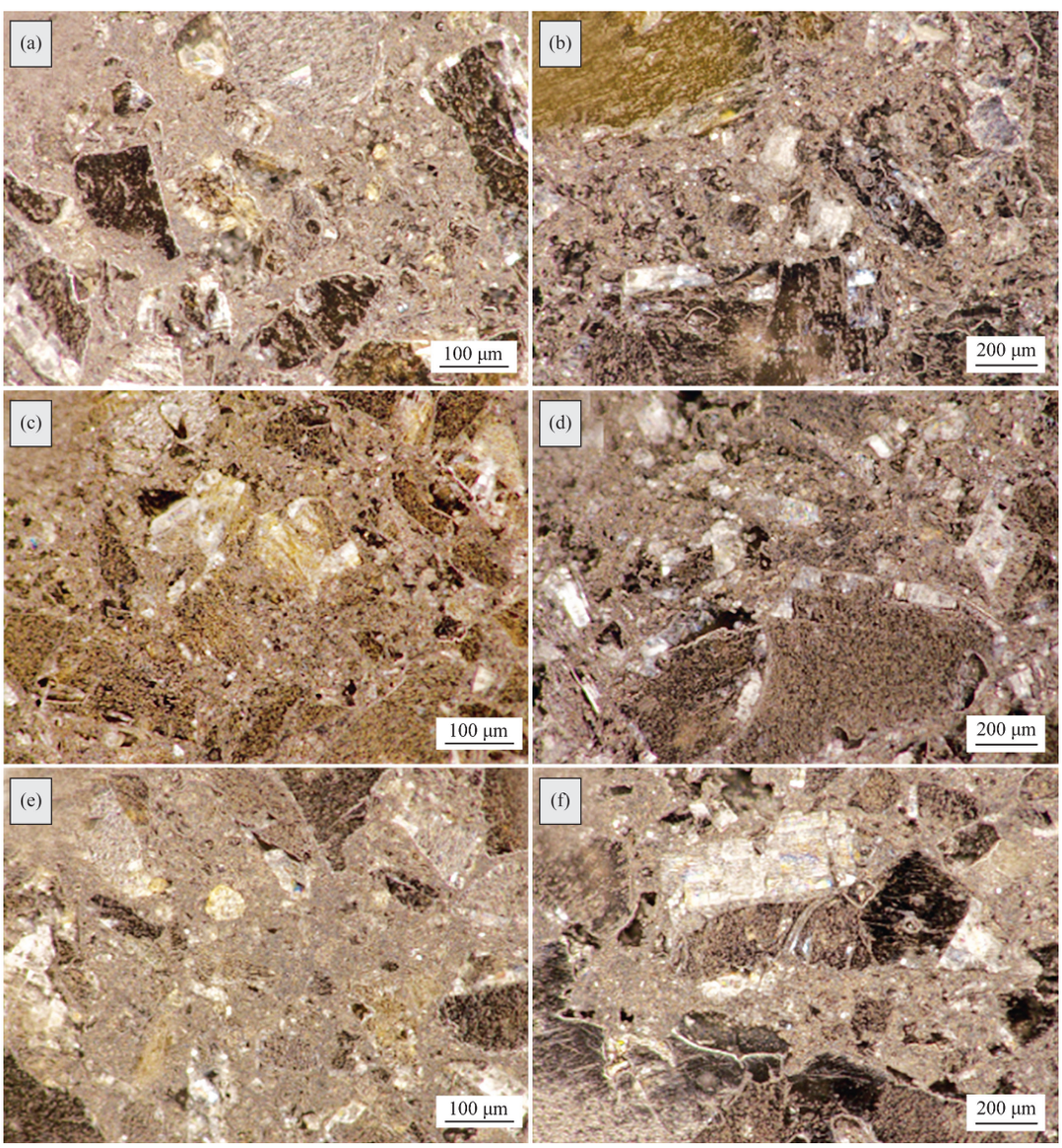

Fig. 1 Light microscope images of sample MgO–C_NFL (a, b), sample MgO–C_WP (c, d), and sample MgO–C_SFSH (e, f), each after pressing (left) and carbonization (right)

received by digital light microscopy at 200-times magnification. The light microscope is not able to distinguish specific differences in the microstructure of the samples, neither after pressing nor after carbonization. Due to the low amount of graphite (<3 *mass*%), the microstructure appearance in the light microscope is dominated by the MgO fractions. All microstructures appear dense without salient defects such as big pores or cracks.

Figure 2 shows the SEM microstructure of the reference sample MgO–C_NFL after pressing (Fig. 2(a)) and carbonization (Fig. 2(b)). In the SEM images, the graphite NFL is identifiable well. With its elongated and lamellar structure, the graphite NFL is flexibly arranged between the MgO grains during pressing with a good integration within the microstructure but is not able to fill finer pores between the oxidic grains. This situation remains after carbonization.

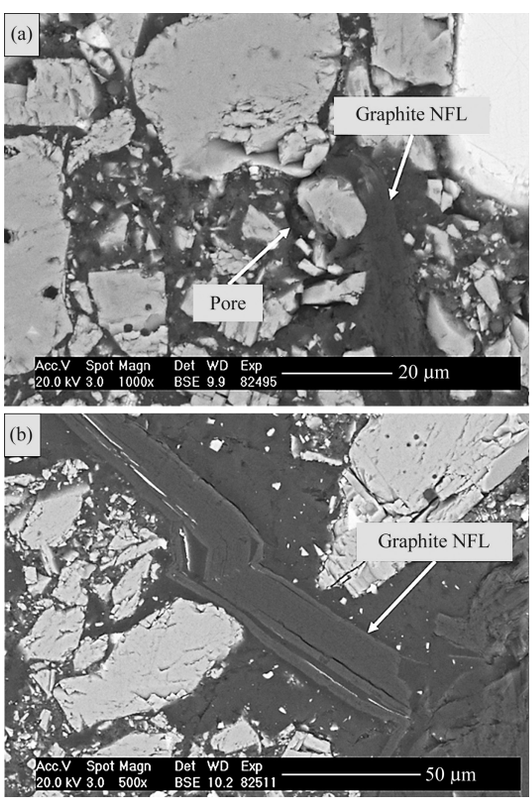

Fig. 2 SEM images (BSE) of sample MgO–C_NFL after pressing (a) and after carbonization (b)

Figure 3 shows the SEM microstructure of the wood pellet coke-containing sample MgO–C_WP, again after pressing (Fig. 3(a)) and carbonization (Fig. 3(b)). As presented in the previous study[12], the carbonized wood pellet is porous, which gets also obvious in Fig. 3. Most of the coke pores were filled with the matrix material during pressing, which explains the comparatively low increase in the apparent porosity in view of comparing the structure of the WP with the dense graphite NFL. However, the WP coke does not behave like a flexible particle such as flaky graphite and hence does not support the arrangement and densification of the oxidic grains, resulting in lower density and strength after pressing as well as a microstructure with some bigger pores. Again, this microstructural character remains after carbonization.

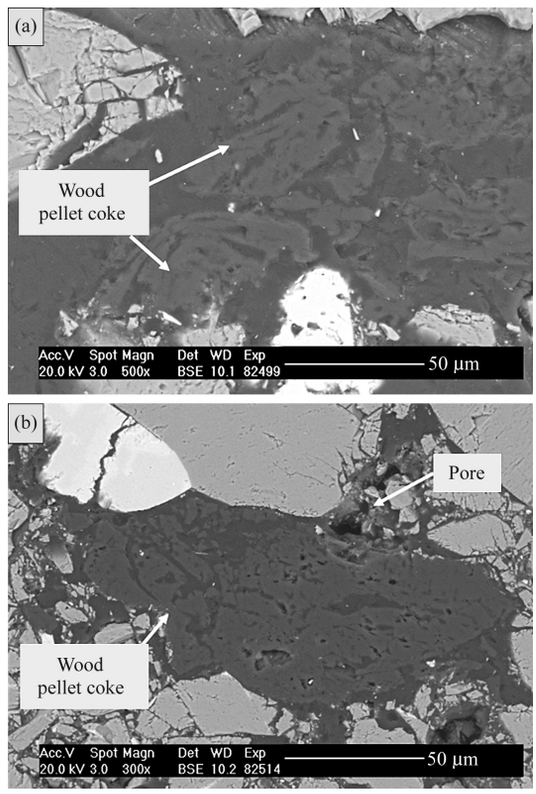

Fig. 3 SEM images (BSE) of sample MgO–C_WP after pressing (a) and after carbonization (b)

Figure 4 displays the SEM microstructure of the sunflower seed hull pellet coke-containing sample MgO–C_SFSH after pressing (Fig. 4(a)) and carbonization (Fig. 4(b)). Similar to the wood pellet coke, the sunflower seed hull pellet coke doesn't support the pressing process but is well incorporated in the microstructure between the oxidic grains. Most of the pores of the SFSH pellet coke are filled with fine matrix material, but compared to the wood pellet coke some of the pores remain unfilled. This explains the higher porosity of the sample MgO–C_SFSH after pressing compared to sample MgO–C_WP. Additionally, similar to sample MgO–C_WP, worse densification compared to the sample containing flaky graphite is indicated by remaining big pores with a size above 50 µm. The microstructure character stays nearly the same after carbonization.

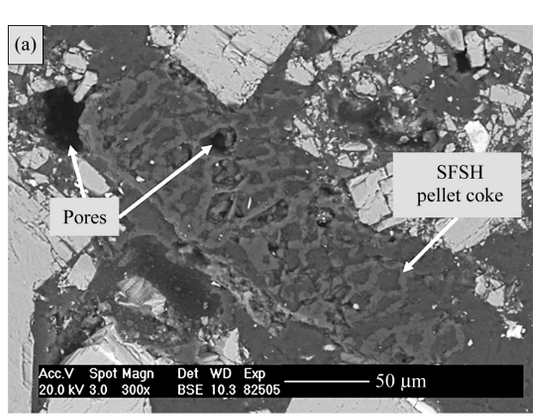

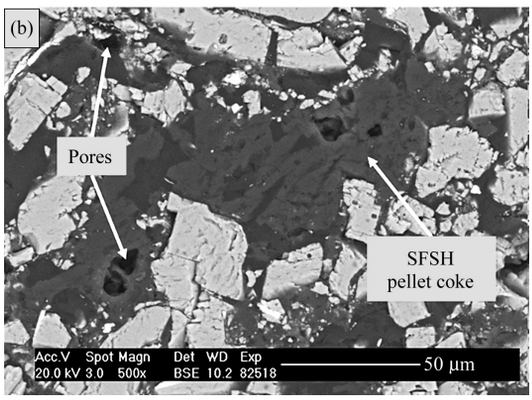

Fig. 4 SEM images (BSE) of sample MgO–C_SFSH after pressing (a) and after carbonization (b)

3.4 Thermal Shock Resistance

Table 4 summarizes the thermal shock (TS) resistance of the MgO–C samples illustrated by the modulus of rupture (MOR) before and after thermal shock. The reference sample with graphite NFL possesses the highest MOR (3.38 MPa) after carbonization. Replacing graphite by the biomass cokes will significantly decrease the MOR to approximately 2 MPa. Quenching the reference sample from 950 °C using air resulted in a loss of MOR of 44% (1.89 MPa). Sample MgO–C_WP showed nearly the same loss of MOR after TS of 43%, which means that disregarding the lower strength value the thermal shock resistance of the wood pellet coke containing MgO–C is at the same level as the reference sample with flaky graphite. However, as sample MgO–C_WP exhibits a lower *E*, the higher porosity of the biomass coke compared to graphite NFL has no distinctive positive effect on the thermal shock resistance compared to the reference sample.

Table 4 MOR before and after thermal shock (TS) from 950 °C

Sample	MOR /MPa		Loss of MOR /%
	Before TS	After TS	
MgO–C_NFL	3.38	1.89	44
MgO–C_WP	2.03	1.16	43
MgO–C_SFSH	2.05	1.05	49

4 Conclusions

(1) The replacement of graphite NFL by carbonized wood and sunflower seed hull pellets marginally reduces the bulk density and increases the apparent porosity after pressing and carbonization.

(2) The replacement of graphite NFL by sunflower seed hull pellet coke does not influence Young's modulus of elasticity after carbonization.

(3) The SEM is appropriate to display the graphite and biomass cokes within the microstructure. All types of carbon are well integrated into the microstructure but cannot actively reduce the pores between the MgO grains, as they do not fill the majority of the pores.

(4) Disregarding the lower strength value, the thermal shock resistance of the wood pellet coke containing MgO–C is at the same level as the reference sample with flaky graphite.

Acknowledgement

This study was funded by the Deutsche Forschungsgemeinschaft (DFG, German Research Foundation), project number 461482547, within the Research Training Group "GRK 2802: Refractory Recycling: A contribution for raw material-, energy- and climate-efficiency in high temperature processes". The authors thankfully acknowledge the support of Dr. Gert Schmidt for the SEM/EDX investigations and Dr. Vânia Regina Salvini (Universidade Federal de São Carlos) for her inspiring input to conduct the thermal shock resistance investigation.

References

[1] Ali Hasanbeigi, Lynn K Price, Aimee T McKane. The state-of-the-art clean technologies (SOACT) for steelmaking handbook. Asia Pacific Partnership for Clean Development and Climate, 2010.

[2] Yuxiang Dai, Jing Li, Wei Yan, Chengbin Shi. Corrosion mechanism and protection of BOF refractory for high silicon hot metal steelmaking process. Journal of Materials Research and Technology, 2020, 9(3): 4292–4308.

[3] W. S. Resende, R. M. Stoll, S. M. Justus, R. M. Andrade, E. Longo, J. B. Baldo, E. R. Leite, C. A. Paskocimas, L. E. B. Soledade, J. E. Gomes, J. A. Varela. Key features of alumina/magnesia/graphite refractories for steel ladle lining. Journal of the European Ceramic Society, 2000, 20(9): 1419–1427.

[4] W. A. Calvo, P. Ortega, M. J. Velasco, V. Muñoz, P. Pena, A. G. Tomba Martinez. Characterization of alumina–magnesia–carbon refractory bricks containing aluminium and silicon. Ceramics International, 2018, 44(8): 8842–8855.

[5] R. I. Services. Natural and Synthetic Graphite: Global Industry Markets and Outlook. Roskill Information Services Limited, 2012. https://books.google.de/books?id=EJxhkQEACAAJ.

[6] Tianbin Zhu, Yawei Li, Shengli Jin, Shaobai Sang, Qinghu Wang, Lei Zhao, Yuanbing Li, Shujing Li. Microstructure and mechanical properties of MgO–C refractories containing expanded graphite. Ceramics International, 2013, 39(4): 4529–4537.

[7] Subham Mahato, Swadesh K. Pratihar, Shantanu K. Behera. Fabrication and properties of MgO–C refractories improved with expanded graphite. Ceramics International, 2014, 40(10): 16535–16542.

[8] Charles A. Schacht. Refractories Handbook. Marcel Dekker, Inc. New York, 2004.

[9] Satyananda Behera, Ritwik Sarkar. Low-carbon magnesia–carbon

refractory: Use of N220 nanocarbon black. International Journal of Applied Ceramic Technology, 2014, 11(6): 968–976.
[10] Tianbin Zhu, Yawei Li, Shaobai Sang, Shengli Jin, Yuanbing Li, Lei Zhao, Xiong Liang. Effect of nanocarbon sources on microstructure and mechanical properties of MgO–C refractories. Ceramics International, 2014, 40(3): 4333–4340.
[11] Liu Bo, Sun Jialin, Tang Guangsheng, Liu Kaiqi, Li Lin, Liu Yongfeng. Effects of nanometer carbon black on performance of low-carbon MgO–C composites. Journal of Iron and Steel Research, International, 2010, 17(10): 75–78.
[12] P. Gehre, A. Kitze, S. Guhl, M. Gräbner, C. G. Aneziris. Carbonized wood and sunflower seed hull pellets as a substitution for carbon black for the production of MgO–C refractories. Open Ceramics, 2024,17: 100550.

Received in June, 2024